ACS APPLIED MATERIALS & INTERFACES

Research Article

www.acsami.org

Template-Free Synthesis of Renewable Macroporous Carbon via Yeast Cells for High-Performance Supercapacitor Electrode Materials

Hongmei Sun, Wenhui He, Chenghua Zong, and Lehui Lu*

State Key Laboratory of Electroanalytical Chemistry, Changchun Institute of Applied Chemistry, Chinese Academy of Sciences, 5625 Renmin Street, Changchun 130022, People's Republic of China

Supporting Information

ABSTRACT: The urgent need for sustainable development has forced material scientists to explore novel materials for next-generation energy storage devices through a green and facile strategy. In this context, yeast, which is a large group of single cell fungi widely distributed in nature environments, will be an ideal candidate for developing effective electrode materials with fascinating structures for high-performance supercapacitors. With this in mind, herein, we present the first example of creating three-dimensional (3D) interpenetrating macroporous carbon materials via a template-free method, using the green, renewable, and widespread yeast cells as the precursors. Remarkably, when the as-prepared materials are used as the electrode materials for supercapacitors, they exhibit outstanding performance with high specific capacitance of 330 F g^{-1} at a current density of 1 A g^{-1}, and good stability, even after 1000 charge/discharge cycles. The approach developed in this work provides a new view of making full use of sustainable resources endowed by nature, opening the avenue to designing and producing robust materials with great promising applications in high-performance energy-storage devices.

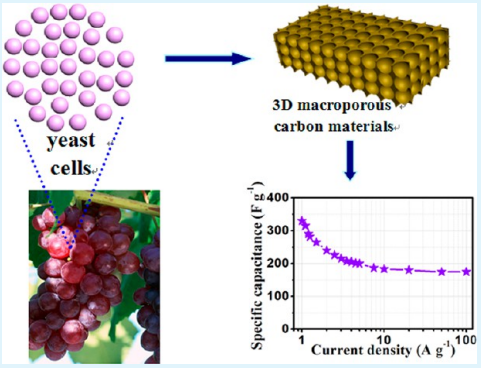

KEYWORDS: *carbon, macroporous materials, structure–property relationships, supercapacitors, template-free approaches*

1. INTRODUCTION

One of the greatest and most important tasks facing the scientific community in the 21st century is to achieve a paradigm shift for the fabrication of materials from the traditional acute way to a green and low-cost approach, to meet the demand for sustainable development.[1−3] In this context, it is required to search for a series of secure, renewable, and sustainable sources as the precursors. Yeasts, which are a large group of single cell fungi, are widely distributed in the nature environments including plant leaves, flowers, and fruits.[4,5] In fact, ∼4000 years ago, yeasts were widely employed as the leavening agent in bakery products and alcoholic fermentation. Based on the above information, on the perspective of materials researchers, we cannot help wondering whether these micro-organisms close to our daily life could open the door to developing the novel materials with amazing structures and fascinating properties?

Currently, a growing global energy demand has driven the exploration of new energy systems.[6] Among those, supercapacitors are considered to be promising candidates, because of their high power performance, long cycle, and low maintenance cost.[6−22] Generally, the design of high-performance supercapacitors is mainly dependent on the development of efficient electrode materials. Carbon materials, from the early activated carbon to mesoporous carbon, carbon nanotubes, and, very recently, graphene, have already been reported to act as the electrode materials for supercapacitors, because of their large surface areas, high electrical conductivity, and low cost.[7−13,20] Despite this progress, the practical use of supercapacitors based on carbon materials is greatly hindered by their low specific capacitance, especially at the high charge/discharge rate.[21] Scientists never give up their attempts to perfect these new energy systems. Recent advances have demonstrated that the electrode materials consisting of three-dimensional (3D) interpenetrating structures, especially 3D interpenetrating macroporous networks, could provide a good solution to the issue by improving the poor ionic transport of electrolytes in electrode materials. Examples include the preparation of 3D graphene networks for supercapacitor applications by using nickel foam as a sacrificial template and the fabrication of 3D macroporous graphene films via a well-known replicating and embossing technique.[18,21] Furthermore, very recently, our group also reported the preparation of 3D macroporous carbon materials for high-performance supercapacitors by the ice template.[3] However, these 3D interpenetrating macroporous carbon materials were generally prepared using a template-directed approach, which involved elaborate synthesis steps. Until now, how to produce 3D interpenetrating macroporous carbon materials though a simple

Received: January 16, 2013
Accepted: March 2, 2013
Published: March 2, 2013

Scheme 1. Schematic Illustration of the Synthesis of 3D Interpenetrating Macroporous Carbon Materials, Taking HYCA-750 °C as an Example

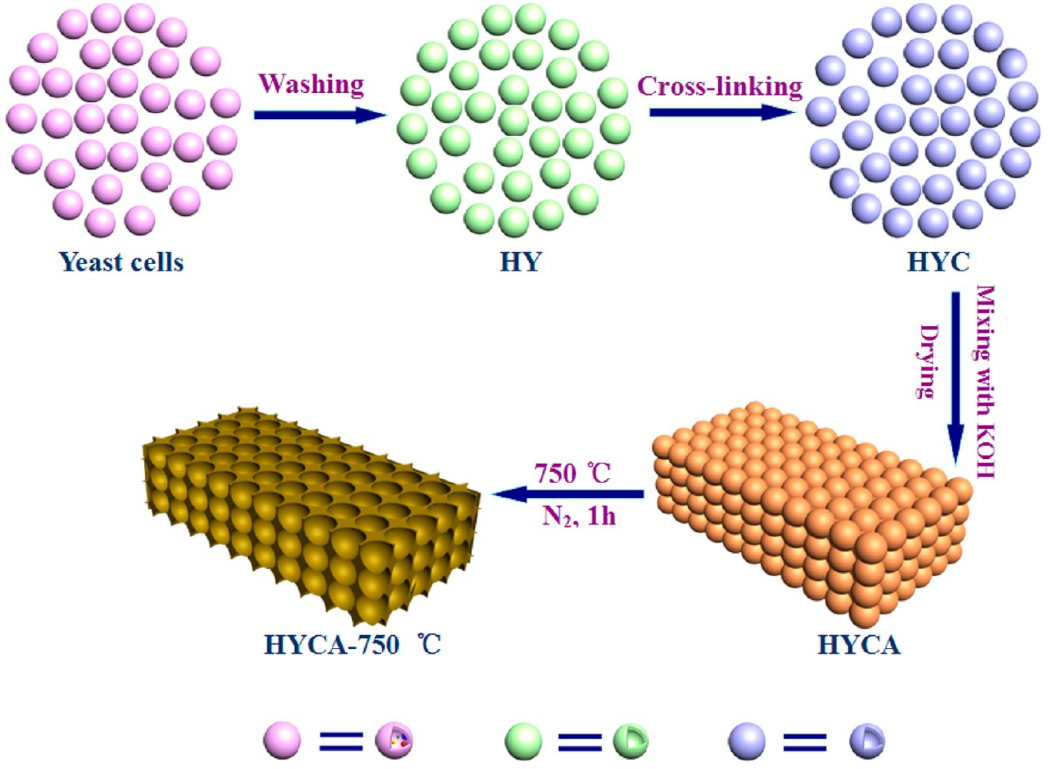

template-free strategy has remained a great challenge, because of the lack of appropriate carbon precursors.

With these in mind, herein, we demonstrate the first example of creating 3D interpenetrating macroporous carbon materials by a template-free strategy using the green, renewable, and widespread yeast cells as the precursors. Importantly, when the as-prepared products are used as the electrode materials for supercapacitors, they exhibit excellent performance with high specific capacitance of 330 F g^{-1} at the current density of 1 A g^{-1}, and good stability even after 1000 charge/discharge cycles.

2. EXPERIMENTAL SECTION

Synthesis. In a typical experiment, 1 g of yeast cells (*S. cerevisiae* cells, purchased from Angel Yeast Co., Ltd., China) was first washed three times with acetone, to remove the protoplast inside the cells, and then dried in an oven at 30 °C for 4 h (the products were denoted as HY). Subsequently, HY were dispersed in the glutaraldehyde aqueous solution (3% (v/v), 100 mL) and stirred for 12 h at room temperature (the products were denoted as HYC). The HYC was centrifuged and washed with distilled water for three times. Then they were mixed with KOH solution (3 g KOH, 50 mL H_2O) and stirred for 2 h. After centrifugation, the precipitate was dried and the HYC/KOH mixture (denoted as HYCA) were obtained. Finally, the HYCA were carbonized under the insert atmosphere at the temperature of 650−850 °C and washed by distilled water, and the final 3D macroporous carbon materials (named as HYCA-temperature) were created.

Characterization. SEM measurement of the samples was investigated using a FEI/Philips XL30 ESEM FEG field-emission scanning electron microscopy (SEM) system. Transmission electron microscopy (TEM) and high-angle annular dark-field scanning TEM (HAADF-STEM) images were recorded on a Hitachi H-8100 TEM system with an accelerating voltage of 200 kV. The effective electron probe size and dwell time used in HAADF-STEM energy-dispersive spectroscopy (EDS) mapping experiments were 1−2 nm and 40 ms per pixel, respectively. Infrared spectra were collected on a VERTEX 70 Fourier transform infrared (FTIR) spectrometer (Bruker). X-ray diffraction (XRD) spectra were obtained using a Bruker D8 ADVANCE diffractometer (Germany) using Cu Kα (1.5406 Å) radiation. The Raman spectrum was obtained using a Renishaw Raman system model 2000 spectrometer. X-ray photoelectron spectroscopy (XPS) measurement was performed on an ESCALAB-MKII spectrometer (VG Co., U.K.) with Al Kα X-ray radiation as the X-ray source for excitation. Nitrogen adsorption and desorption isotherms were measured at 77 K with a Quadrachrome adsorption instrument. Thermogravimetric analysis (TGA) curves of the samples were performed on a Pyris Diamond TG/DTA thermogravimetric analyzer (Perkin−Elmer Thermal Analysis). Samples were heated under a N_2 atmosphere from room temperature at a rate of 5 °C min^{-1}. Mercury intrusion test was performed with a Micromeritics AutoPore IV 9500 Series pore size analyzer.

Electrochemical Measurements. In a three-electrode electrochemical cell, the reference electrode and the counter electrode were Ag/AgCl and Pt, respectively. The suspension of the materials with a concentration of 2.0 mg mL^{-1} was prepared by ultrasonically dispersing them (10 mg) in a mixture (5 mL) of ethanol and Nafion. The suspension (5 μL) was then dropped onto the glassy carbon electrode and dried thoroughly in air. The glassy carbon electrode coated with the as-prepared materials was used as the working electrode and 1 M KOH was used as the electrolyte. Cyclic voltammograms and galvanostatic charge/discharge curves of the samples were measured by a CHI 660D electrochemical workstation (Shanghai CH Instruments Co., China). Electrochemical impedance spectroscopy (EIS) measurements were carried out with Solartron 1255B frequency response analyzer (Solartron, Inc., U.K.). The frequency range for the impedance spectra was from 0.01 Hz to 150 kHz with a voltage amplitude of ±10 mV. All the electrochemical tests were performed in a three-electrode system, except that in Figure S9 in the Supporting Information. In Figure S9 in the Supporting Information, a symmetrical two-electrode electrochemical cell was fabricated to get the galvanostatic charge/discharge curves of HYCA-750 °C.

dx.doi.org/10.1021/am400206r | ACS Appl. Mater. Interfaces 2013, 5, 2261−2268

3. RESULTS AND DISCUSSION

The strategy for the fabrication of 3D interpenetrating macroporous carbon materials was schematically illustrated in Scheme 1. First, raw yeast cells were washed with acetone, to remove the protoplast inside the cells (the products were named as HY; see Figures S1a–c in the Supporting Information).[23] Subsequently, glutaraldehyde was used to act as a cross-linking agent through covalently bonding to aldehyde or amide groups in the polysaccharide networks of yeast cell wall (the cross-linked HY were denoted as HYC; see Figures S1d and S1e in the Supporting Information).[4] Then, HYC was mixed with KOH to form a HYC/KOH mixture (denoted as HYCA). Finally, 3D interpenetrating macroporous carbon materials were produced by a simple carbonization of HYCA under insert atmosphere (named as HYCA-temperature).

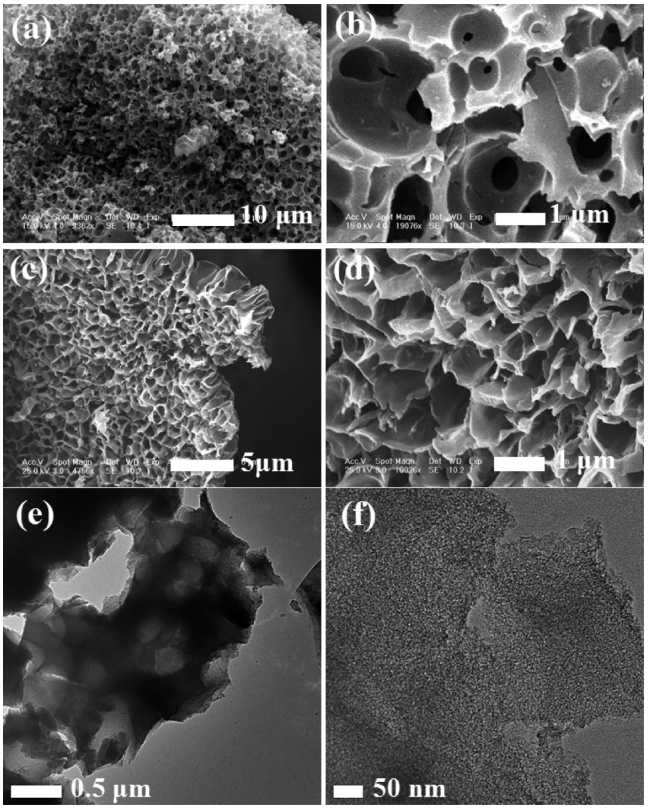

Figure 1. (a–d) Scanning electron microscopy (SEM) and (e,f) transmission electron microscopy (TEM) images of HYCA-750 °C.

Figures 1a and 1c showed SEM images of the as-prepared products. It was noted that these materials possessed the characteristic 3D open porous architectures, as well as a monolithic shape. At higher magnification, another interesting feature was evident, i.e., the pores with sizes ranging from submicrometer to several micrometers were interconnected and not simply and completely separated (see Figures 1b and 1d). Such structural features were further confirmed by TEM images (Figure 1e). A closer examination revealed that the walls of 3D macroporous carbon materials were composed of highly disordered wormlike pores with diameters ranging from a few nanometers to tens of nanometers (see Figure 1f). These pores in nanometer scale could have resulted from the KOH activation process and the pyrolysis of the yeast cell walls at high temperature.[24]

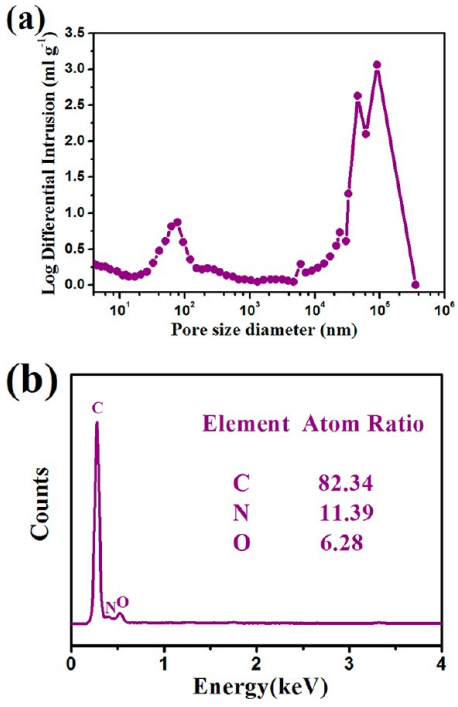

Figure 2. (a) Pore size distribution of HYCA-750 °C measured by mercury porosimetry. (b) Energy-dispersive X-ray (EDX) analysis of HYCA-750 °C.

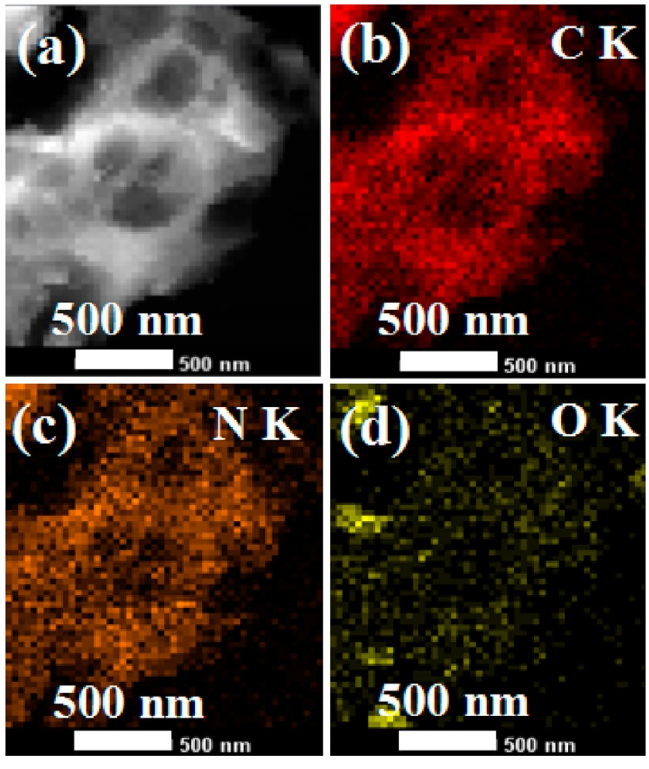

Figure 3. (a) High-angle annular dark-field scanning TEM (HAADF-STEM) image of HYCA-750 °C; (b–d) energy-dispersive spectroscopy (EDS) mapping images of C, N, O of HYCA-750 °C.

More direct evidence for the formation of macroporous structures was provided by mercury intrusion analysis. It clearly revealed that the as-prepared materials possessed abundant mesopores (2–50 nm) and macropores (>50 nm) (Figure 2a).

dx.doi.org/10.1021/am400206r | ACS Appl. Mater. Interfaces 2013, 5, 2261–2268

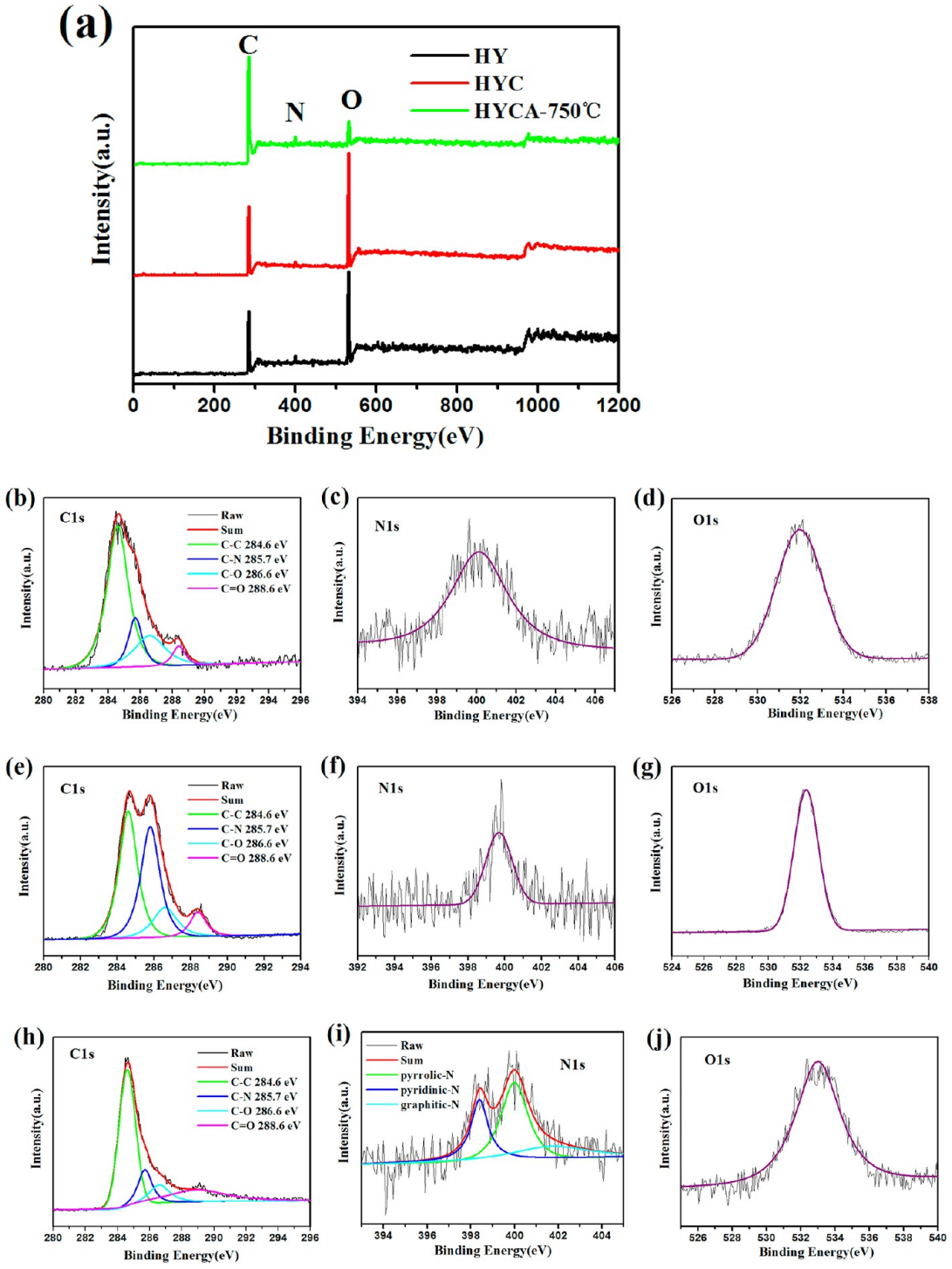

Figure 4. The total XPS spectra of (a) HY, HYC, and HYCA-750 °C, and C 1s, N 1s, and O 1s spectra of (b–d) HY, (e–g) HYC, and (h–j) HYCA-750 °C.

Such features would be beneficial to the ion diffusion and the contact of electrode materials with electrolyte, thus leading to high performance when they were used as the electrode materials for supercapacitors.[3,18,21] The porous architectures of the as-prepared materials were further verified by a high-angle annular dark-field scanning TEM (HAADF-STEM) image (Figure 3a). In particular, the HAADF-STEM EDX mapping images clearly showed that a large amount of N and O elements were uniformly distributed in the 3D carbon materials (Figures 3b–d), indicating the existence of abundant foreign atoms in the as-prepared materials. This result was very consistent with the energy-dispersive X-ray (EDX) analysis (see Figure 2b).

The structure and composition of the materials were investigated by means of FTIR spectroscopy, XRD, and Raman spectroscopy. FTIR spectrum of HYCA-750 °C showed a dramatic decrease in the intensity of absorption bands assigned to the oxygen functional groups, compared with that of HY and HYC, indicating that most of the oxygen functional groups were removed after carbonization.[25−27] Moreover, the appearance of the absorption band at 1580−1650 cm^{-1},

dx.doi.org/10.1021/am400206r | ACS Appl. Mater. Interfaces 2013, 5, 2261−2268

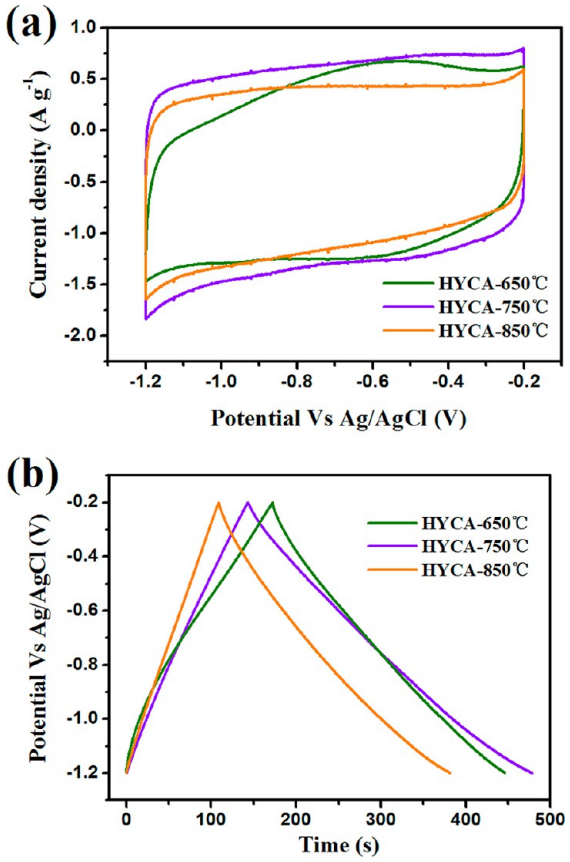

Figure 5. (a) Cyclic voltammetry (CV) curves at 5 mV s^{-1} and (b) galvanostatic charge/discharge curves at 1 A g^{-1} of the samples.

corresponding to the C═C stretching vibration, demonstrated the aromatization of HYCA during the carbonization process (see Figure S2a in the Supporting Information).[4] These features would be propitious to improve the electronic conductivity of the as-prepared materials.[3] The XRD pattern of the final materials (Figure S2b in the Supporting Information) showed two characteristic peaks, located at ~25° and ~43°, which could be indexed to the (002) and (100) planes of graphite, respectively.[28] However, the broad and low intensity of the peaks indicated that the as-prepared materials possessed a low degree of graphitization.[29] The typical Raman spectrum of HYCA-750 °C exhibited two remarkable Raman shifts—a broad D band (peak at 1375 cm^{-1}) and a G band (peak at 1609 cm^{-1})—suggesting the appearance of a high degree of structural disorder in the 3D carbon materials associated with the porous structures (see Figure S2c in the Supporting Information).[30]

XPS was then used to determine the surface chemical properties of the 3D interpenetrating macroporous carbon materials.[25−27] The fully scanned spectrum of the final product demonstrated three peaks, at 284.8, 399.6, and 531.9 eV, corresponding to C 1s, N 1s, and O 1s, respectively, further confirming the existence of abundant foreign atoms in HYCA-750 °C (Figure 4a).[30] To understand the electronic states of the elements, we paid more attention to the higher-resolution spectra. A deconvoluted C 1s spectrum of the as-prepared material was fitted with four peaks. The main peak at 284.6 eV could be assigned to sp^2 hybridized carbon, indicating that most of C atoms are aromatic carbon (Figure 4h).[24] It was well in agreement with the FTIR results. The N 1s spectrum of HYCA-750 °C had three components: the pyridinic nitrogen at 398.4 eV, the pyrrolic/pyridinic nitrogen at 400.1 eV, and the graphitic nitrogen at 401.7 eV (Figure 4i).[31] It was noteworthy that the peak intensity of graphitic nitrogen was weaker than that of pyridinic nitrogen and pyrrolic/pyridinic nitrogen, implying that pyridinic nitrogen and pyrrolic nitrogen were dominant in the as-prepared materials. The pyridinic and pyrrolic nitrogens located at the edge of the carbon materials induced more disorders of the final carbon materials, well elucidating the phenomena for the broad D band in Raman spectrum.[30]

To shed light on the possible formation mechanism of the final products, we conducted a series of control experiments. It was noted that both cross-linking and mixing with KOH were crucial for the successful fabrication of 3D macroporous carbon materials. On the one hand, if the yeast cells were treated under the same conditions but without mixing with KOH, only microspheres ~2 μm in size were obtained (denoted as HYC-750 °C; see Figure S3a in the Supporting Information). On the other hand, if the precursors were not cross-linked by glutaraldehyde, the products exhibited relatively disordered structures with fragmented carbon materials (denoted as HYA-750 °C; see Figure S3b in the Supporting Information). Moreover, TGA also revealed that HYC had better thermal stability than HY (see Figure S4 in the Supporting Information). These results indicated that the cross-linking by glutaraldehyde could efficiently enhance the strength of the polysaccharide networks of the yeast cell wall, thus avoiding the undesired breaking.[4] In addition, previous studies demonstrated that KOH had been widely used on the activation of carbon nanotubes, graphene, carbon nanofibers, and biomasses to obtain porous carbon materials.[10,20,24,28] It was suggested that the activation of carbon with KOH proceeded as $6KOH + C \leftrightarrow 2K + 3H_2 + 2K_2CO_3$, followed by decomposition of K_2CO_3 and/or reaction of $K/K_2CO_3/CO_2$ with carbon.[10] Furthermore, during the activation process, KOH could also change the original structures of the precursors. For example, it could change microspheres to irregularly shaped platelets.[20] Based on the above discussions, the mechanism for transforming the precursors to the final 3D macroporous carbon material was rationalized as follows. Under high-temperature conditions, the carbonization and the activation of carbon occurred. During this process, KOH could integrate the walls of two hollow yeast cells abutting each other to form the 3D interpenetrating macroporous carbon materials. Importantly, thanks to the cross-linking process, the precursors were substantial enough to ensure the construction of the final 3D interpenetrating macroporous carbon materials, other than the irregular structures.

It is known that the carbonization temperature of materials has an important influence on their electrochemical behavior.[32] Prior to using the products as the electrode materials for supercapacitors, we first optimized the carbonization temperatures. SEM images of HYCA-650 °C and HYCA-850 °C showed no obvious difference from that of HYCA-750 °C (Figure S5 in the Supporting Information). However, the cyclic voltammograms (CV) and galvanostatic charge/discharge experiments revealed that HYCA-750 °C had the largest encircled area and longest discharge time, implying that HYCA-750 °C had the best capacitance behavior (Figure 5).[33] The specific capacitance of HYCA-750 °C measured was calculated to be 330 F g^{-1} at a current density of 1 A g^{-1}, according to the discharge time, via the following equation:

dx.doi.org/10.1021/am400206r | ACS Appl. Mater. Interfaces 2013, 5, 2261−2268

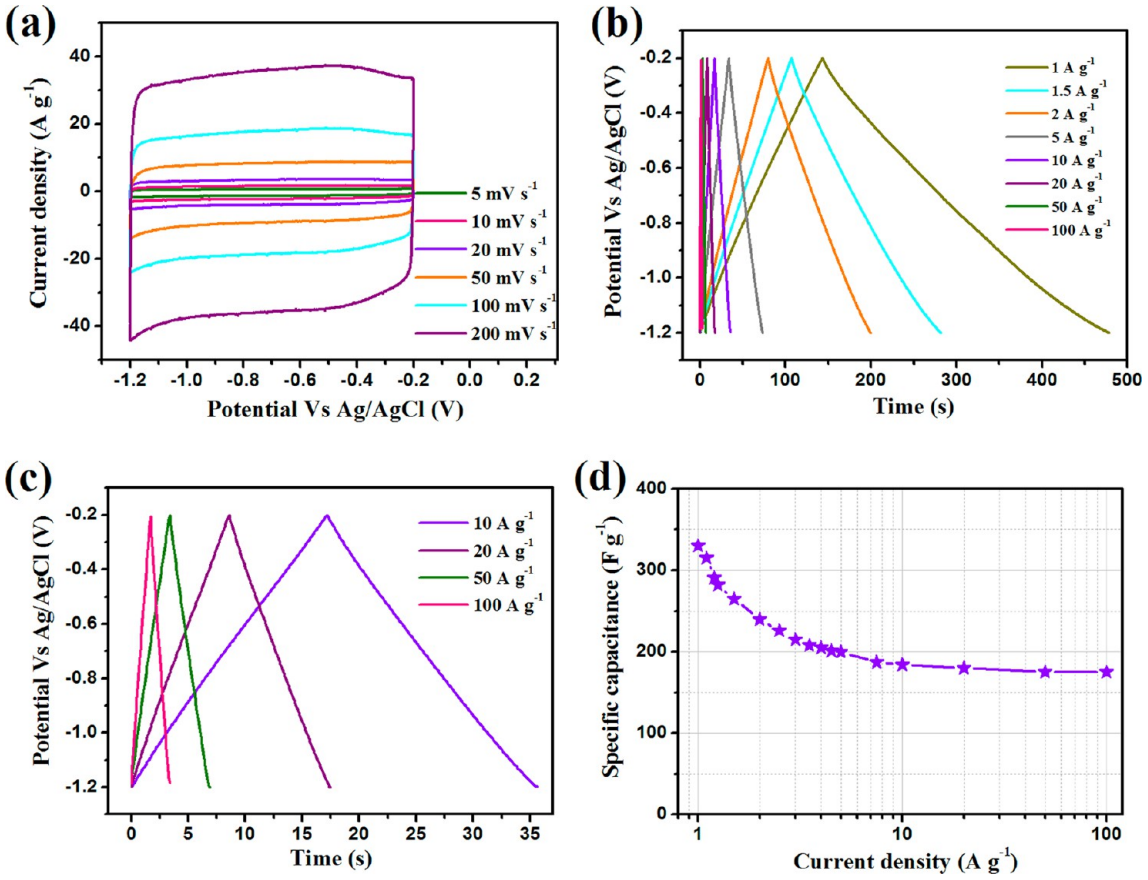

Figure 6. (a) CV curves and (b) galvanostatic charge/discharge curves of HYCA-750 °C at different scan rates and current densities, respectively; panel c shows a magnified view of the short time range in panel b, and panel d shows the specific capacitance of HYCA-750 °C at different current densities.

$$C = \frac{I\Delta t}{\Delta V m} \quad (1)$$

where I is the applied current, Δt the discharge time, ΔV the potential drop during discharge, and m the mass of electrode material.[34] The value was higher than that of HYCA-650 °C (276 F g^{-1}), HYCA-850 °C (274 F g^{-1}), HYC-750 °C (115 F g^{-1}; see Figure S6 in the Supporting Information), HYA-750 °C (284 F g^{-1}; see Figure S6 in the Supporting Information), the previously reported 3D graphene networks (163 F g^{-1}), and other carbon materials.[3,7,20,32,33]

To ascertain the origin of the exceptional performance of HYCA-750 °C, nitrogen adsorption/desorption measurement was conducted (see Figure S7 and Table S1 in the Supporting Information). Generally, the sample with larger surface area exhibited higher performance.[32] It could give a good reason for higher specific capacitance of HYCA-750 °C (with a surface area of 1227 m^2 g^{-1}) than that of HYCA-650 °C (with a surface area of 1002 m^2 g^{-1}). However, it could not explain the low performance of HYCA-850 °C (with a surface area of 2011 m^2 g^{-1}). Previous reports demonstrated that elemental nitrogen and oxygen would considerably improve the wettability of electrode materials with electrolytes, as well as introduce large additional pseudo-capacitance through the faradic reactions at the electrode interfaces.[3,35] Inspired by this, we turned to investigate the compositions of the samples. EDX analysis revealed that HYCA-750 °C contained a larger amount of foreign atoms than HYCA-850 °C (see Figure 2b, as well as Figure S8 and Table S2 in the Supporting Information). Hence, we concluded that the lower specific capacitor of HYCA-850 °C, compared with that of HYCA-750 °C, might be attributed to the reduction of foreign atoms (N and O) with the increase of carbonization temperature.

As stated above, HYCA-750 °C as electrode materials exhibited a specific capacitance as high as 330 F g^{-1} (280 F g^{-1} when measured by two-electrode system; see Figure S9 in the Supporting Information), we thus proceeded to investigate the electrochemical properties of HYCA-750 °C in details. All CV curves of HYCA-750 °C presented a rectangular-like shape without a very oblique angle, even at a scan rate of 200 mV s^{-1} (Figure 6a). Furthermore, the voltage−time (V−t) curves of HYCA-750 °C were all similar to a linear shape within the potential window between −1.2 V and −0.2 V (see Figures 6b and 6c). They were in accordance with the performance of the electrical double-layer capacitors.[7,11] Importantly, the as-prepared material possessed good rate capability and a specific capacitance of 175 F g^{-1} could be obtained, even at a fast charge/discharge rate of 100 A g^{-1} (Figure 6d). It suggested that the as-prepared material had great promise in practical applications.

The excellent electrochemical behavior of HYCA-750 °C was further confirmed by the electrochemical impedance spectroscopy (EIS) analysis and the cycle stability measurement (Figure 7). The Nyquist plot showed a straight line in the low-frequency region and an arc in the high-frequency region. The projected length of the Warburg-type line (the slope of 45° portion of the curve) on the real axis was short, implying fast ion diffusion in the 3D interpenetrating macroporous carbon

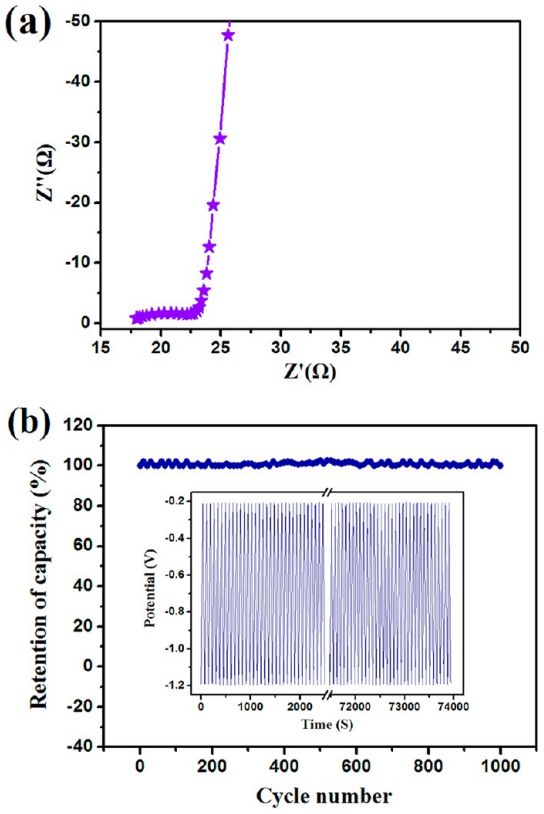

Figure 7. (a) Nyquist plots of experimental impedance data of HYCA-750 °C electrode; (b) cycle stability of the HYCA-750 °C electrode in 1 M KOH (current density of 5 A g^{-1}). The inset in panel b shows the 1000 charge/discharge cycles.

materials.[11] In addition, in the high-frequency region, the intercept of the semicircle with the real axis was also very short, indicating the excellent operation rate of the capacitor.[35] Furthermore, the charge/discharge cycle stability experiment showed that the specific capacitance had no obvious decreases, even after 1000 cycles at the current density of 5 A g^{-1}. It was probably due to the superior structural stability of the as-prepared 3D materials (see the SEM image shown as Figure S10 in the Supporting Information).

4. CONCLUSIONS

In summary, a novel, facile, template-free strategy had been proposed to prepare three-dimensional (3D) macroporous carbon materials using the green, renewable, and widespread yeast cells as the precursors. It was found that the steps including cross-linking and activation with KOH have an important influence on the morphology and structure of the final products. Importantly, when used as the electrode materials for supercapacitors, the as-prepared 3D interpenetrating macroporous carbon materials exhibited excellent electrochemical properties with high specific capacitance of 330 F g^{-1} at a current density of 1 A g^{-1}, and good stability even after 1000 charge/discharge cycles. The approach that was developed in this work provided a good example for making full use of a series of sustainable resources endowed by nature, opening the avenue for designing and producing a variety of novel materials with great promising applications in high-performance energy storage devices.

■ ASSOCIATED CONTENT

Supporting Information

Additional characterization data (XPS, XRD, Raman spectra, FTIR, EDX, N_2 adsorption/desorption isotherms, SEM images). This material is available free of charge via the Internet at http://pubs.acs.org.

■ AUTHOR INFORMATION

Corresponding Author

*Tel.: (+86) 431-85262418. Fax: (+86) 431-85262406. E-mail: lehuilu@ciac.jl.cn.

Notes

The authors declare no competing financial interest.

■ ACKNOWLEDGMENTS

Financial support by NSFC (No. 21125521), the National Basic Research Program of China (973 Program, No. 2010CB933600) and the "Hundred Talents Project" of the Chinese Academy of Science is gratefully acknowledged.

■ REFERENCES

(1) Anastas, P.; Warner, J. *Green Chemistry: Theory and Practice*; Oxford University Press: New York, 1998.
(2) Dahl, J. A.; Maddux, B. L. S.; Hutchison, J. E. *Chem. Rev.* **2007**, *107*, 2228−2269.
(3) Sun, H. M.; Cao, L. Y.; Lu, L. H. *Energy Environ. Sci.* **2012**, *5*, 6206−6213.
(4) Ni, D.; Wang, L.; Sun, Y.; Guan, Z.; Yang, S.; Zhou, K. *Angew. Chem., Int. Ed.* **2010**, *49*, 4223−4227.
(5) Shen, W.; He, Y.; Zhang, S.; Li, J.; Fan, W. *ChemSusChem* **2012**, *5*, 1274−1280.
(6) Wang, G.; Zhang, L.; Zhang, J. *Chem. Soc. Rev.* **2012**, *41*, 797−828.
(7) Hulicova-Jurcakova, D.; Puziy, A. M.; Poddubnaya, O. I.; Suárez-García, F.; Tascón, J. M. D.; Lu, G. Q. *J. Am. Chem. Soc.* **2009**, *131*, 5026−5027.
(8) Feng, D.; Lv, Y.; Wu, Z.; Dou, Y.; Han, L.; Sun, Z.; Xia, Y.; Zheng, G.; Zhao, D. *J. Am. Chem. Soc.* **2011**, *133*, 15148−15156.
(9) Futaba, D. N.; Hata, K.; Yamada, T.; Hiraoka, T.; Hayamizu, Y.; Kakudate, Y.; Tanaike, O.; Hatori, H.; Yumura, M.; Iijima, S. *Nat. Mater.* **2006**, *5*, 987−994.
(10) Zhu, Y.; Murali, S.; Stoller, M. D.; Ganesh, K. J.; Cai, W.; Ferreira, P. J.; Pirkle, A.; Wallace, R. M.; Cychosz, K. A.; Thommes, M.; Su, D.; Stach, E. A.; Ruoff, R. S. *Science* **2011**, *332*, 1537−1541.
(11) Yang, X.; Zhu, J.; Qiu, L.; Li, D. *Adv. Mater.* **2011**, *23*, 2833−2838.
(12) Zheng, G.; Hu, L.; Wu, H.; Xie, X.; Cui, Y. *Energy Environ. Sci.* **2011**, *4*, 3368−3373.
(13) Guo, C. X.; Li, C. M. *Energy Environ. Sci.* **2011**, *4*, 4504−4507.
(14) Milczarek, G.; Inganäs, O. *Science* **2012**, *335*, 1468−1471.
(15) Wang, H.; Casalongue, H. S.; Liang, Y.; Dai, H. *J. Am. Chem. Soc.* **2010**, *132*, 7472−7477.
(16) Su, F.; Poh, C. K.; Chen, J. S.; Xu, G. N.; Wang, D.; Li, Q.; Lin, J.; Lou, X. W. *Energy Environ. Sci.* **2011**, *4*, 717−724.
(17) Wu, Z.; Wang, D.; Ren, W.; Zhao, J.; Zhou, G.; Li, F.; Cheng, H. *Adv. Funct. Mater.* **2010**, *20*, 3595−3602.
(18) Cao, X.; Shi, Y.; Shi, W.; Lu, G.; Huang, X.; Yan, Q.; Zhang, Q.; Zhang, H. *Small* **2011**, *7*, 3163−3168.
(19) Zhai, Y.; Dou, Y.; Zhao, D.; Fulvio, P. F.; Mayes, R. T.; Dai, S. *Adv. Mater.* **2011**, *23*, 4828−4850.
(20) Wei, L.; Sevilla, M.; Fuertes, A. B.; Mokaya, R.; Yushin, G. *Adv. Funct. Mater.* **2012**, *22*, 827−834.
(21) Choi, B. G.; Yang, M. H.; Hong, W. H.; Choi, J. W.; Huh, Y. S. *ACS Nano* **2012**, *6*, 4020−4028.

(22) Li, Z.; Zhang, L.; Amirkhiz, B. S.; Tan, X.; Xu, Z.; Wang, H.; Olsen, B. C.; Holt, C. M. B.; Mitlin, D. *Adv. Energy Mater.* **2012**, *2*, 431−437.
(23) Ashkenazy, R.; Gottlieb, L.; Yannai, S. *Biotechnol. Bioeng.* **1997**, *55*, 1−10.
(24) Xing, W.; Liu, C.; Zhou, Z.; Zhang, L.; Zhou, J.; Zhuo, S.; Yan, Z.; Gao, H.; Wang, G.; Qiao, S. *Energy Environ. Sci.* **2012**, *5*, 7323−7327.
(25) Sun, H. M.; Cao, L. Y.; Lu, L. H. *Nano Res.* **2011**, *4*, 550−562.
(26) He, W. H.; Lu, L. H. *Adv. Funct. Mater.* **2012**, *22*, 2542−2549.
(27) Ai, K. L.; Liu, Y. L.; Lu, L. H.; Cheng, X. L.; Huo, L. H. *J. Mater. Chem.* **2011**, *21*, 3365−3370.
(28) Qie, L.; Chen, W.; Wang, Z.; Shao, Q.; Li, X.; Yuan, L.; Hu, X.; Zhang, W.; Huang, Y. H. *Adv. Mater.* **2012**, *24*, 2047−2050.
(29) White, R. J.; Tauer, K.; Antonietti, M.; Titirici, M. M. *J. Am. Chem. Soc.* **2010**, *132*, 17360−17363.
(30) Mao, Y.; Duan, H.; Xu, B.; Zhang, L.; Hu, Y.; Zhao, C.; Wang, Z.; Chen, L.; Yang, Y. *Energy Environ. Sci.* **2012**, *5*, 7950−7955.
(31) Feng, L.; Chen, Y.; Chen, L. *ACS Nano* **2011**, *5*, 9611−9618.
(32) Xie, K.; Qin, X.; Wang, X.; Wang, Y.; Tao, H.; Wu, Q.; Yang, L.; Hu, Z. *Adv. Mater.* **2011**, *24*, 347−352.
(33) Zhu, H.; Wang, X.; Yang, F.; Yang, X. *Adv. Mater.* **2011**, *23*, 2745−2748.
(34) Zhang, L. L.; Zhao, X. S. *Chem. Soc. Rev.* **2009**, *38*, 2520−2531.
(35) Xu, B.; Yue, S.; Sui, Z.; Zhang, X.; Hou, S.; Cao, G.; Yang, Y. *Energy Environ. Sci.* **2011**, *4*, 2826−2830.